Experiments in Fluids 20 (1996) 395–397 © Springer-Verlag 1996

Generation of nearly isotropic turbulence using two oscillating grids

A. Srdic, H. J. S. Fernando, L. Montenegro

Abstract Isotropic turbulence has unique properties and is impracticable to realize experimentally. Past experiments in this context have been performed by passing a uniform mean flow through a grid, which yields approximately isotropic decaying turbulence. Here an alternative approach of obtaining approximately isotropic stationary turbulence is described, which utilizes two monoplanar grids oscillating in a homogeneous fluid. It was found that the central region between the grids has certain properties similar to that of isotropic turbulence.

1 Introduction

Isotropic turbulence is the simplest class of turbulent flows, in that a minimum number of quantities and relations are required to describe it. To an extent, isotropic turbulence is amenable to theoretical treatment and provides an essential building block to the understanding of more complex inhomogeneous flows. Yet, in practical point of view, these flows are hypothetical because no actual flows can satisfy the conditions for isotropy. The best one can do is to generate flows in which conditions for isotropy are more or less approached. Some of these properties are: $\overline{u_1^3}=\overline{u_2^3}=\overline{u_3^3}=0$, $\overline{u_i u_j}=0$, and $\overline{u_1^2}=\overline{u_2^2}=\overline{u_3^2}$, where u_1, u_2 and u_3 are fluctuating velocities in x, y and z directions. In general, however, turbulent flows having these properties are in a decaying state, and their practical utility is limited.

In the past, most of the experimental studies on isotropic turbulence have been performed by passing a uniform mean flow through a grid (e.g., Mohamed and LaRue 1990) or dropping a grid through a stagnant fluid layer (Dickey and Mellor 1980). When properly designed, these configurations provide nearly isotropic decaying flow, the turbulent statistics of which can be measured using suitable techniques. Because of the rapid decay of turbulence, however, it is impracticable to use such configurations to study certain important aspects such as particle or scalar dispersion in isotropic turbulent flows, without compromising the accuracy and versatility. In this note we describe an attempt to generate nearly isotropic sustained (stationary) turbulence, which can be conveniently adopted for many experimental studies. Like wind tunnel techniques, this technique also only yields approximately isotropic turbulence and only a limited number of requirements for isotropy is satisfied.

The present work is based on the findings of DeSilva and Fernando (1993) that the oscillating grid turbulence indeed has some local properties characteristic of isotropic turbulence. In their investigation, a single oscillating grid was used, and the resulting turbulence was found to decay with the distance from the grid ξ as (Hopfinger and Toly 1976)

$$(\overline{u_1^2})^{1/2},\ (\overline{u_3^2})^{1/2} \propto S^{3/2} M^{1/2} f \xi^{-1} \tag{1}$$

where S is the stroke, M is the mesh size, f is the frequency of oscillations (in Hz) and ξ is the distance measured from the grid. It was further found that $(\overline{u_1^2})^{1/2}/(\overline{u_3^2})^{1/2}=1.2$, $\overline{u_1^3}\approx 0$ and $\overline{u_1 u_3}\approx 0$, indicating that the turbulence tends to have some properties of isotropic turbulence, in local sense (here u_1 is measured in the direction of grid oscillations). The advantage of this flow configuration over wind tunnel techniques is the stationarity of the flow and the compactness of the apparatus. Although this flow configuration can be used in studies such as the decay of isotropic turbulence (by shutting off the grid oscillations), for investigations involving the dispersion of substances the turbulence should be locally isotropic and homogeneous over an appreciable spatial domain. To this end, it was decided to utilize a two-grid configuration, having parallel grids oscillating out of phase, with the hope that the spatially decaying turbulence of both grids may interact to form a substantial approximately isotropic turbulent region in between the grids.

2 Experimental Method

Figure 1 shows a schematic of the experimental apparatus. It is a glass box of interior dimensions 58 × 36 × 36 cm. The grids are fitted vertically at either end of the tank, and the distance between a grid plane and the closest end wall is 7 cm, thus allowing a mean distance of 44 cm between the grids. The

Received: 27 March 1995/*Accepted*: 11 November 1995

A. Srdic, H. J. S. Fernando, L. Montenegro
Environmental Fluid Dynamics Program and Department of Mechanical and Aerospace Engineering, Arizona State University, Tempe, AZ 85287-6106, USA

Correspondence to: H. J. S. Fernando

The funding for the particle dispersion studies at Arizona State University (ASU) is provided by the Environmental Protection Agency (Office of Exploratory Research). The stratified and rotating flow research at ASU is funded by the Office of Naval Research and the National Science Foundation.

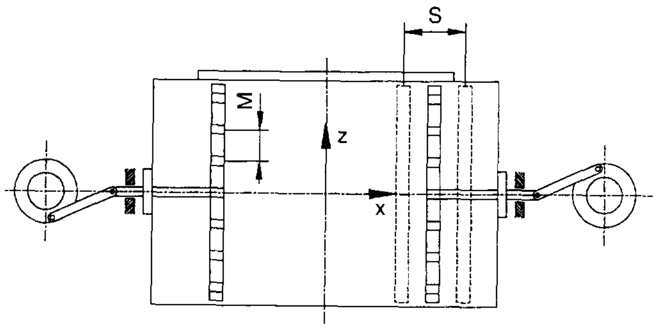

Fig. 1. A schematic diagram of the experimental apparatus

stainless steel grids are made of 1 cm square bars with a mesh of size 5 cm solidity 38%, and provisions are made to obtain strokes up to 5.5 cm. In the design of the apparatus, precautions were taken to minimize the secondary circulation in the tank; these considerations are described in DeSilva and Fernando (1993, 1994). The grids could be oscillated out of phase with speeds up to 5 Hz, and their rectilinear oscillatory motion was ensured by constraining the connecting rods to move along guide rails and precision bearings. The top surface of the tank was fitted with a lid to reduce surface waves generation. The velocity measurements were made using a two-component fiber optic Laser Doppler Velocimeter (Dantec model 5490A-00) in forward-scattering mode. Typical data rate and validation rate were 200 Hz and 12% and the sampling time was 100 s. The turbulence was measured along the x axis at various locations in y–z planes; the coordinate system used is shown in Fig. 1. Standard data reduction techniques were employed to calculate the turbulence statistics. Statistical properties were calculated by averaging over a period of 100 s.

3 Results and Conclusions

The normalized r.m.s. velocity $(\overline{u_1^2})^{1/2}$ and $(\overline{u_3^2})^{1/2}$ measurements along the x axis for two different frequencies are presented in Fig. 2. Here the distance has been normalized by the half-distance between the grids, $D=22$ cm, and fS was selected as the velocity scale. The data corresponding to the single grid oscillations are indicated by the dashed lines for the u_1 component and solid lines for the u_3 component. Typically $(\overline{u_1^2})^{1/2}/(\overline{u_3^2})^{1/2} \approx 1.2$–$1.5$.

The two spatially decaying velocity fields of individual grids have interacted to yield a nearly homogeneous field in the middle part of the tank. Note that the flow cannot be completely homogeneous, because to supply kinetic energy to the midpart of the tank the energy flux divergence should be nonzero; in fact the scale of inhomogeneity is expected to be on the order of the integral length scale. This behavior is typical of all experiments, although the velocity fields near the grids did not show consistent decay behaviour in different experiments perhaps due to the presence of some secondary mean flow. The interesting fact here is the unusual amplification of $(\overline{u_3^2})^{1/2}$, when both grids are in motion, possibly due to the "stagnation effect" of the flow. Each grid produces a bias effect in the u_1 direction (the direction of oscillations) and these effects are compensated when both grids are present. During this interaction, stagnation-point type flows can be generated thus enhancing the u_3 component.

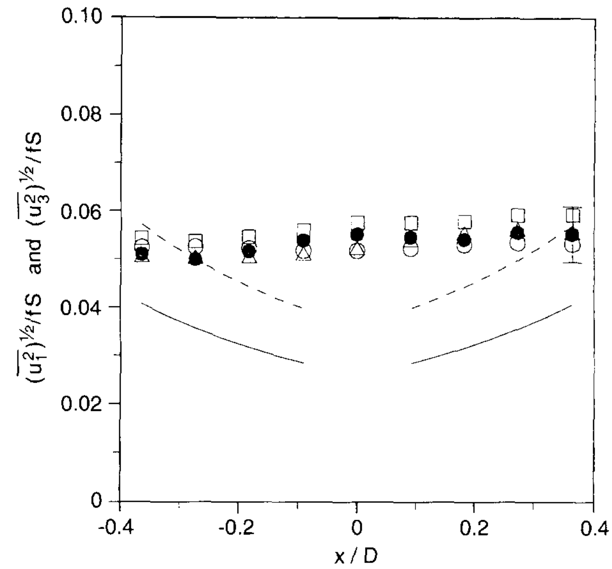

Fig. 2. A plot of the non-dimensional r.m.s. velocities $(\overline{u_1^2})^{1/2}$ and $(\overline{u_3^2})^{1/2}$ vs. normalized distance x/D: $f=3$ Hz, $S=2$ cm, $M=5$ cm, (●) $(\overline{u_1^2})^{1/2}$, (□) $(\overline{u_3^2})^{1/2}$; $f=4$ Hz, $S=2$ cm, $M=5$ cm, (○) $(\overline{u_1^2})^{1/2}$, (△) $(\overline{u_3^2})^{1/2}$ (measurements were made along the x axis)

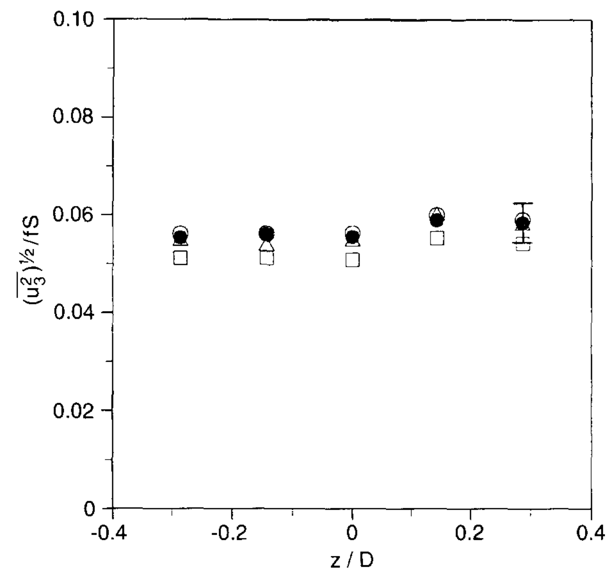

Fig. 3. Measurements of $(\overline{u_3^2})^{1/2}$ along the z axis, which show approximate vertical homogeneity in the central region of the tank. (△) $f=4$ Hz, $x/D=0.2$; (●) $f=3$ Hz, $x/D=0.0$; (□) $f=4$ Hz, $x/D=0.0$; (○) $f=3$ Hz, $x/D=0.2$

Figure 3 shows an example of the vertical z distribution of the $(\overline{u_3^2})^{1/2}$ component at $x/D=0$ and $x/D=0.2$, which also demonstrates the vertical homogeneity surrounding the middle region between the grids. Similar trend was observed for $(\overline{u_1^2})^{1/2}$. Various other properties of turbulence in this region are depicted in Fig. 4. These include the mean velocities between the grids ($\bar{U}_1$ and $\bar{U}_3$); the ratio of the vertical to horizontal r.m.s. velocities $(\overline{u_3^2})^{1/2}/(\overline{u_1^2})^{1/2}$; the normalized third

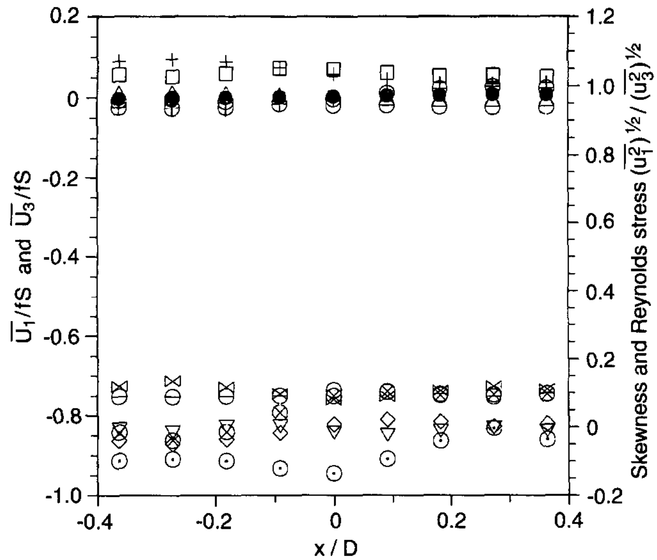

Fig. 4. A plot that summarizes various properties of turbulence, measured along the x axis: $f=3$ Hz, $S=2$ cm, $M=5$ cm, (●) $\bar{U}_1$, (○) $\bar{U}_3$, (□) $(\overline{u_1^2})^{1/2}/(\overline{u_3^2})^{1/2}$, (◇) $\overline{u_1^3}/(\overline{u_1^2})^{3/2}$, (⊖) $\overline{u_3^3}/(\overline{u_3^2})^{3/2}$, (⊙) $-\overline{u_1 u_3}/(\overline{u_1^2}\,\overline{u_3^2})^{1/2}$; $f=4$ Hz, $S=2$ cm, $M=5$ cm, (△) $\bar{U}_1$, (⊕) $\bar{U}_3$, (+) $(\overline{u_1^2})^{1/2}/(\overline{u_3^2})^{1/2}$, (▽) $\overline{u_1^3}/(\overline{u_1^2})^{3/2}$, (⋈) $\overline{u_3^3}/(\overline{u_3^2})^{3/2}$, (⊗) $-\overline{u_1 u_3}/(\overline{u_1^2}\,\overline{u_3^2})^{1/2}$

order moments of velocity (skewness), $(\overline{u_1^3})/(\overline{u_1^2})^{3/2}$ and $(\overline{u_3^3})/(\overline{u_3^2})^{3/2}$; and, the Reynolds stress $-\overline{u_1 u_3}/(\overline{u_1^2}\,\overline{u_3^2})^{1/2}$. These results show that for most of the time the secondary mean circulation in the tank is weak but not completely absent. In some cases, its magnitude can be as high as 30% of the r.m.s. velocity and this secondary circulation remains the bane of all oscillating grid experiments. The integral lengthscales were not measured in the present experiments but could be calculated using $l=(\overline{u_1^2})^{1/2}/\tau$ where τ is the integral time scale. The results show that within $\pm 10\%$, l is uniform in the central region of the tank with $l \approx 0.1D$. By and large, in the central region of the tank, $-0.1<x/D<0.1$, the normalized third order moments and Reynolds stresses are small on the order 0.1, but not completely absent. It is possible to assume $(\overline{u_1^2})^{1/2}/(\overline{u_3^2})^{1/2} \approx 1$, $(\overline{u_1^3})/(\overline{u_1^2})^{3/2} \approx 0$, $(\overline{u_3^3})/(\overline{u_3^2})^{3/2} \approx 0$, and $-\overline{u_1 u_3}/(\overline{u_1^2}\,\overline{u_3^2})^{1/2} \approx 0$, indicating that for practical purposes the turbulence produced by the two-grid configuration can be considered as approximately isotropic. In the future, it is planned to use this apparatus (with appropriate modifications) for the studies of neutrally buoyant particle dispersion and settling of heavy particles in isotropic turbulent flows.

References

Dickey JD; Mellor GL (1980) Decaying turbulence in neutral and stratified fluids. J Fluid Mech 99: 13–31

DeSilva IPD; Fernando HJS (1993) Note on secondary flows in oscillating-grid, mixing-box experiments. Phys Fluids A 5: 1849–1851

DeSilva IPD; Fernando HJS (1994) Oscillating grids as a source of nearly isotropic turbulence. Phys Fluids 6: 2455–2464

Hopfinger EJ; Toly JA (1976) Spatially decaying turbulence and its relation to mixing across density interfaces. J Fluid Mech 78: 155–175

Mohamed MS; LaRue JC (1990) The decay power law in grid-generated turbulence. J Fluid Mech 219: 195–214